Study of undisturbed loess stress-strain experiments based on CT

Zhaoyang Wang

College of Geology & Environment, Xi'an University of Science and Technology, Xi'an, China

wangzhaoyang1999@126.com

Keywords: undisturbed loess; damage; stress-strain.

Abstract. Test method for observation of geotechnical material in structural damage has become one of the hot field of mechanics, which is the basis to establish the structural model. The authors use real time CT test of triaxial stress in undisturbed loess during triaxial shear tests - strain were studied. The paper analyzes the Q_2 and Q_3 loess stress - strain curves, proposed initial damage stress undisturbed loess method of determining the threshold of strain. Based on the test results, it indicates Q_2 compared Q_3 depressed loess prone to injury at low confining, and its strain injury threshold lower than the Q_3 loess. On this basis, the damage variable formula proposed by the number of CT defined fitting draw damage variable axial strain and deviatoric stress relationship. CT triaxial test instrument can reveal undisturbed loess structural damage evolution and deformation and destruction law. The instrument is a powerful tool for in-depth analysis of the mechanical properties of the soil.

Introduction

In recent years the micro, meso and macro tests proved the geotechnical material is a natural damage material. The core issues of the 21st century soil mechanics is a mathematical model of soil structural（Shen. 1996）. Test method for observation of geotechnical material in structural damage has become one of the hot field of mechanics, which is the basis to establish the structural model. Liu et al., (2005) has established the Lanzhou frozen loess uniaxial compression damage constitutive model by using the dynamic CT test. Lu et al., （2002） used the CT machine supporting of unsaturated triaxial apparatus, the dynamic, quantitative and without damage research on unsaturated undisturbed expansive soil in triaxial shear test process, which test soil samples obtained internal structural damage clearly Ctimages and corresponding data. Huang et al., (2004) studied the mechanical properties of red clay under triaxial stress conditions using CT technology. Under triaxial stress conditions Sun et al., (2005) tested chacteristics of Shanghai clay by means of a CT machine.

CT technology has the following advantages (Chen et al., 2001): ①change dynamically, quantitative and non-destructive measurements of the internal structure of the material in the course of the force; ②get a thin layer density distribution, there is the problem of overlapping objects around defects , and three-dimensional objects into a different sheet in accordance with image data; ③ large detection area and high resolution. which the resolution is the main indicator of CT machine performance. CT machine spatial resolution in this article is 0.35 mm×0.35 mm, volume resolution of 0.12 mm^3 (thickness 1 mm), the density contrast resolution of 0.3% (3 HU).

CT triaxial test of undisturbed loess

The use of state key laboratory of frozen soil engineering CT apparatus, undisturbed loess was undrained shear tests, while the sample section CT scan, observe internal structural changes . The soil samples for the Q_3, Q_2 undisturbed loess, with undisturbed sample is made of soil height of 12.5 cm, 6.18 cm diameter sample.

In triaxial pressure chamber, undisturbed loess were first prepared consolidation, to be stable deformation, triaxial shear test. Shear rate is 0.3 mm / min. After the consolidation is complete and in the initial state of the sample, the sample were three layers of scanning of 2%, 5%, 8%, 10% and 19% of each stage. Three aliquots of the scanning position in the sample, and track scanning section scanning, location divided into three sections. Before shearing the basic parameters of soil samples and test conditions are shown in table 1. During the scanning process scans each corresponding stress - strain state in table 2.

Table 1 Initial conditions and parameters before shear test

soil	ρ / (g/cm^3)	w / %	p / kPa
Q_2 loess	1.61	15.82	70
Q_3 loess	1.44	13.89	70

Table 2 Stress-strain data of each scanning

Strain/ %	q / kPa	
	Q_3 loess	Q_2 loess
2	118.32	313.13
5	201.76	329.91
8	241.85	394.21
10	272.00	414.56
19	387.83	549.25

stress - strain analysis and determination of damage variable

Stress - strain analysis

Deviatoric stress and axial strain curves of undisturbed loess shown in figure 1.

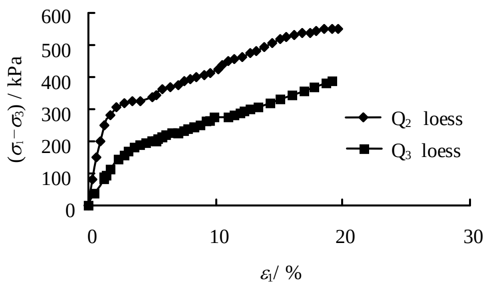

Fig .1 deviatoric stress versus strain of Q_3 and Q_2 loesses under 70 kPa confining pressure

As can be seen from the figure 1, undisturbed Q_3 loess stress - strain curve is a tough type of stress - strain curve, the deformation curve Q_2 loess weak hardening stress - strain curve, both plastic failure. Q_2 loess intensity was significantly higher than Q_3, which is due to Q_2 loess dense structure, high bond strength due to the particles.

Q_3 undisturbed loess stress - strain relations

For Q_3 undisturbed loess, available in the form of a power function curve fitting test, then:

$$(\sigma_1-\sigma_3)=\beta\varepsilon_1^{\alpha} \qquad (1)$$

Different tangent modulus stress level E_t

$$E_t=\frac{d(\sigma_1-\sigma_3)}{d\varepsilon_1}=\beta\alpha\varepsilon_1^{\alpha-1}=\alpha\beta^{\frac{1}{\alpha}}(\sigma_1-\sigma_3)^{1-\frac{1}{\alpha}} \qquad (2)$$

Where α and β are experimental constants, functions as the confining pressure σ_3. The test data $(\sigma_1-\sigma_3)$ and ε_1 are plotted in double logarithmic coordinates, as shown in fig 2. The relationship is approximately a straight line, $\lg\beta$ and α respectively, the linear slope distance and gradient.

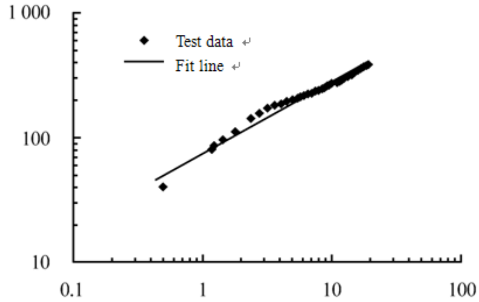

Fig.2 $\lg(\sigma_1-\sigma_3)$ **versus** $\lg\varepsilon_1$

Figure. 2 shows $\beta = 6.57\times10^7$, $\alpha = 0.69$. Therefore tangent modulus $E_t = 4.53\times10^7\varepsilon_1^{-0.31}$.

Q_2 undisturbed loess stress - strain relations

For Q_2 undisturbed loess, stress - strain curves

$$(\sigma_1-\sigma_3)=\frac{\varepsilon_1}{a+b\varepsilon_1} \tag{3}$$

The formula can also be written as

$$\frac{\varepsilon_1}{(\sigma_1-\sigma_3)}=a+b\varepsilon_1 \tag{4}$$

Tangent modulus of different stress levels E_t

$$E_t=\frac{d(\sigma_1-\sigma_3)}{d\varepsilon_1}=\frac{a}{(a+b\varepsilon_1)^2} \tag{5}$$

a and b are experimental constants as a function of σ_3. The test data are plotted in the coordinate system conversion $\varepsilon_1/(\sigma_1-\sigma_3)$ and ε_1, approximately linear relationship, as shown in fig. a and b respectively, the linear intercept and slope.

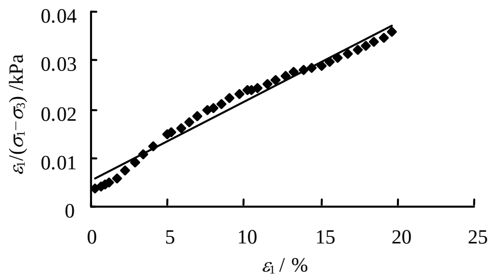

Fig.3 $\varepsilon_1/(\sigma_1-\sigma_3)$ **versus** ε_1

Figure 3 shows $a = 0.0054$, $b = 0.0016$. Therefore tangent modulus is expressed as:

$$E_t=\frac{0.0054}{(0.0054+0.0016\varepsilon_1)^2} \tag{6}$$

Determination of initial damage threshold of stress and strain

Based on the stress-strain curves (Figure 1), there is a turning point marken circle which hints that it is possible to find out the initial damage point. At the initial loading stage, strain increase slowly, and then it increase rapidly with the increase in the stress after coming to turing point, plotted in the half-logarithm coordinate.

The Q_3 and Q_2 undisturbed loess triaxial test results, coming ε_1 - $\lg(\sigma_1-\sigma_3)$ curve (Figure 4,5), which consists of some gentle curves and a steep drop straight lines. The point O is taken as the smallest radius of curvature, the point C is the intersection point of two tangents, and the bisector of angle $\angle$OCB is CD. Then, the point D is considered as an initial damage point and the corresponding stress and strain are called the initial damage threshold of stress and strain.

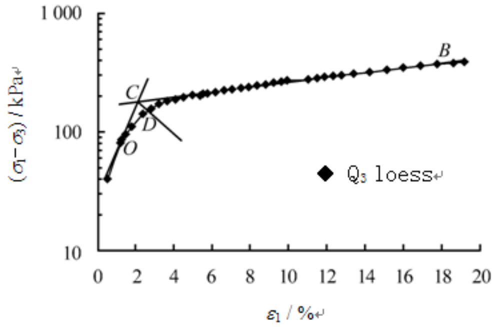

Fig .4 ε_1 versus $\lg(\sigma_1-\sigma_3)$ of Q_3 loess

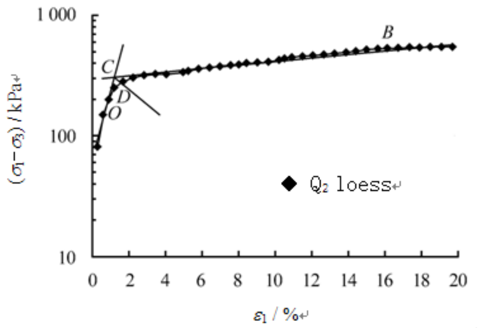

Fig .5 ε_1 versus $\lg(\sigma_1-\sigma_3)$ of Q_2 loess

According to the above method, Q_3 test soil samples to determine the initial bias stress damage is 160 kPa, and strain threshold value is 2.6%. Q_2 initial sample bias stress damage is 280 kPa, and strain threshold value is 1.6%.

Test Q_3 and Q_2 soil overburden gravity stress were 90 and 300 kPa, belongs normally consolidated soil. Confining pressure during the test to maintain 70 kPa, soil damage occurs and the axial stress Q_2 and Q_3 loess were 230 and 350 kPa via the initial stress values. Experimental results show that the initial damage stress of loess is greater than the weight of overburden stress, which when added to the initial damage Q_3 loess axial stress is far greater than the overlying weight stress. This is because the Q_3 loess density, loose structure, more large pores. The beginning of the pressing Q_3 compacted soil produced only soil particles are not shear displacement, its structure remained unchanged damage occurs. Q_2 loess is density, while confining pressure test is small, the axial stress exceeds the overburden gravity stress a little, soil particles shear displacement occurs. Thus, Q_2 loess is more prone to damage in the low confining pressure and strain threshold damage occurs correspondingly smaller.

Determination of damage variable

CT numbers variation of geotechnical materials under stress state can indicate the damage of the material. It can be established by the appropriate constitutive model to establish the relationship between CT number and damage variables.

First, we need derive the absorption coefficient μ and CT number of relationships. Set ρ to material density, then:

$$\mu_{\mathrm{m}} = \frac{\mu}{\rho} \tag{7}$$

Where μ_{m} is the mass attenuation coefficient through 1 g substance; μ is a linear attenuation coefficient of a substance through 1 cm. Hounsfield British professor gives a definition CT numberss(Hounsfield et al., 1973).

$$H = \frac{\mu - \mu_w}{\mu_w} \times 1\,000 \tag{8}$$

Where μ_w is the absorption coefficient of water, the water is concerned, $\rho = 1$

Based on Eqs. (8), H can be expressed as

$$H = \frac{\mu - \mu_w}{\mu_w} \times 1000 = \left(\frac{\mu}{\mu_w} - 1 \right) \times 1000 \tag{9}$$

Based on $\mu_w = 1$, there:

$$H = (\mu - 1) \times 1\,000 \tag{10}$$

$$\mu = \frac{H}{1000} + 1 \tag{11}$$

Mass attenuation coefficient of the mixture(Qiang, 2011):

$$\mu_m = \mu_{m1}\rho_1 + \mu_{m2}\rho_2 + \cdots\cdots + \mu_{mi}\rho_i \tag{12}$$

The formula: ρ_i wherein the weight percentage of a certain component; component μ_{mi} is a mass attenuation coefficient. Ray attenuation coefficient of the mixture can be written as:

$$\mu = \rho \sum_{i=1}^{m} (\mu_{mi}\rho_i) \tag{13}$$

Soil absorption coefficient is expressed as:

$$\mu = \rho(\rho_1\mu_1 + \rho_2\mu_w) = \rho\left(\frac{1}{1+\omega}\mu_1 + \frac{\omega}{1+\omega}\mu_w \right) = \gamma_d(\mu_1 + \omega\mu_w) \tag{14}$$

Substituting Eq.(14) into (10), we have:

$$H = [\gamma_d(\mu_1 + \omega) - 1] \times 1000 \tag{15}$$

Where: Equation ω is the water content of soil samples, γ_d soil samples of dry bulk density. According to the known statistical Q_3 loess scan data to calculate the absorption coefficient Q_3 loess particles (soil samples 5.5 cm) were initially 1.3046, to 1.4299 after the trial.

Bellion et al.,(1978) proposed by the rate of change in the density of the material creep damage of $\Delta\rho / \rho$ to reflect the damage, and the mass conservation law proved the damage variable D can be expressed as

$$D = -\frac{\Delta\rho}{\rho_0} \tag{16}$$

Davis (1966), Lemaitre (1978) and Belloni (1979), and so have to define damage variable material density measurement with damage, but the main difficulty is the amount of change is difficult to measure the density of $\Delta\rho$. Since the application of CT scanning equipment, to solve this problem.

Based on Eqs. (7), $\frac{\Delta\rho}{\rho_0}$ can be expressed as

$$\frac{\Delta\rho}{\rho_0} = \frac{\Delta\mu}{\mu_0} = \frac{\mu_i - \mu_0}{\mu_0} \tag{17}$$

Based on Eqs. (11),

$$\mu_i = \frac{H_i}{1\,000} + 1 \tag{18}$$

$$\mu_0 = \frac{H_0}{1\,000} + 1 \tag{19}$$

$$\frac{\Delta\rho}{\rho_0} = \frac{H_i - H_0}{H_0 + 1\,000} \tag{20}$$

Therefore, the definition of loess damage variable

$$D = -\frac{H_i - H_0}{H_0 + 1\,000} \tag{21}$$

Where H_0 is the initial soil sample damage sectional CT number ME; ME value reflects the average density of all the material points of the selected area. H_i is a cross-sectional CT test average number ME i stages.

In order to facilitate changes of injury variables, taking the absolute value of the formula (21)

$$D_{\mathrm{ME}} = \left| \frac{H_0 - H_i}{H_0 + 1\,000} \right| \tag{22}$$

Where D_{ME} is the damage variable by CT computed ME.

By Eqs. (22) calculated the damage variable is actually a relative value, its exact size of the initial sample size depends on soil tests. This paper selects Q_2 and Q_3 loess initial state average of CT scan three numbers section, as the initial state of the soil damage this test sectional CT number H_0. Curve test soil damage variable values calculated in Figure 6-9.

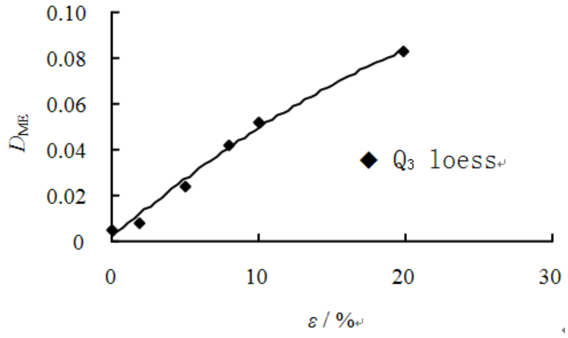

Fig .6 Damage variable D_{ME} versus axial strain of loess Q_3

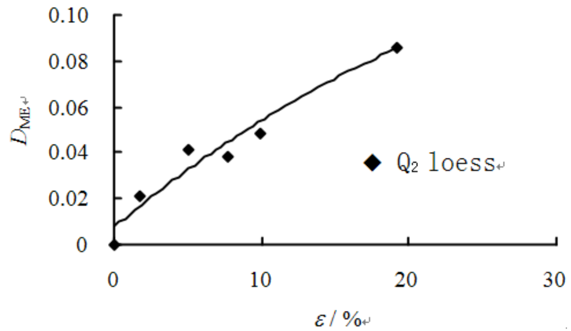

Fig .7 Damage variable D_{ME} versus axial strai of loess Q_2

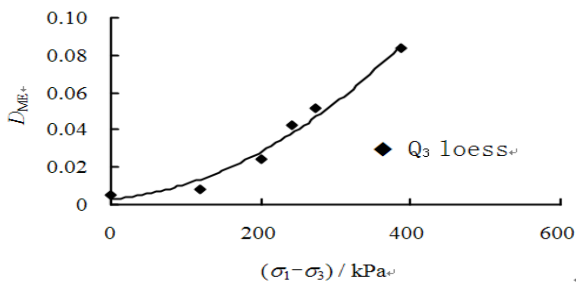

Fig .8 Damage variable D_{ME} versus deviatoric stress of loess Q_3

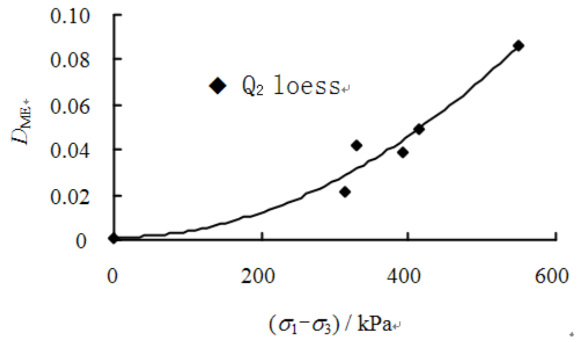

Fig .9 Damage variable D_{ME} versus deviatoric stress of loess Q_2

According to the results, we can draw damage fitting a variable axial strain and deviatoric stress relation

（1） Q_3 loess

$$D_{ME} = -7.0\times10^{-5}\varepsilon_1^2 + 0.0055\varepsilon_1 + 0.0016 \quad (23)$$

$$D_{ME} = 5.0\times10^{-7}(\sigma_1-\sigma_3)^2 + 3.0\times10^{-5}(\sigma_1-\sigma_3) + 0.0029 \quad (24)$$

（2） Q_2 loess

$$D_{ME} = -6.0\times10^{-5}\varepsilon_1^2 + 0.0053\varepsilon_1 + 0.0077 \quad (25)$$

$$D_{ME} = 3.0\times10^{-7}(\sigma_1-\sigma_3)^2 - 2.0\times10^{-6}(\sigma_1-\sigma_3) + 0.0012 \quad (26)$$

Eqs. (23) and (24) are loess damage variable expression of the strain and stress of bias, the result is equivalent to the same for the Eqs. (25) and (26) are also equivalent. As can be seen from Figure 6-9, with the axial strain and deviatoric stress increases, soil damage variable increases. Loess damage variable and partial stress diagram, the two curves are reflected on a concave shape, initial damage value significantly greater than Q_2 and Q_3 loess, while damage variable Q_3 loess and partial stress curve steeper slope large, reflect Q_3 loess in the role of a partial change in stress injuries faster. In the same bias stress, Q_3 loess damage variable value is significantly greater than Q_2 loess. This reflects Q_3 loess loose structure, prone to distortion and shear failure faster.

Conclusion

This paper analyzes the Q_3 and Q_2 undisturbed loess damage process by triaxial testing based on real time CT. This paper r obtained the following conclusions.

（1） CT triaxial test instrument can reveal undisturbed loess structural damage evolution and deformation and destruction law. The instrument is a powerful tool for in-depth analysis of the mechanical properties of the soil.

（2） Q_2 compared Q_3 depressed loess prone to injury at low confining, and its strain injury threshold lower than the Q_3 loess.

（3） Bias stress and strain threshold initial damage of the soil can be obtained by curve ε_1 and $\lg(\sigma_1-\sigma_3)$.

（4） Based on CT number undisturbed loess damage variable can be quantitatively reflect the degree of damage to the soil, Thus laying foundation for further study of the soil damage constitutive model.

References

[1] Zhu-jiang Shen. Mathematical model for soil mass structure —core problem of soil mechanics in the 21st century. Chinese Journal of Geotechnical Engineering, 1996, 18(1): 95－97.

[2] Zeng-li Liu, Xiao-peng Zhang, Hongsheng Li. A damage constitutive model for frozen soils under uniaxial compression based on CT dynamic distinguishing. Rock and Soil Mechanics, 2005, 26(4): 542－546.

[3] Zai-hua Lu, Zheng-han Chen, Yi-bin Pu. Study on damage evolution of natural expansive soil with computerized tomography during triaxial shear test. Journal of Hydraulic Engineering, 2002, (6): 106－112..

[4] Zhi-hong Huang, Li-jun Zhu, Yi-bin Pu, et al. CT analysis of dynamic change of mechanical properties of red clay under triaxial stress. Rock and Soil Mechanics, 2004, 25(8): 1215－1219.

[5] Hong Sun, Xiu-run Gg, Fu-jun Niu, et al. Real-time CT meso-testing on Shanghai silty clay subjected to triaxial loading. Chinese Journal of Rock Mechanics and Engineering, 2005, 24(24): 4559－4564.

[6] Zhen-han Chen, Zai-hua Lu, Yi-bin Pu. The matching of computerized tomograph with triaxial test apparatus for unsaturated soils. Chinese Jounal of Geotechnical Engineering, 2001, 23(4): ： 387－392.

[7] Hounsfield G N. Computerized transverse axial scanning(tomography). British: The British Institute of Radiology, Stanford Libraries, 1973,46: 1016-1022.

[8] Tian-peng Qiang. Radiographic Inspection. Kunming: Yunnan Science & Technology Press, 2001.

[9] BELLION G, BERNASCOIN G. In creep of engineering. Material & Structure, 1978, 8(3): 54－65.

[10] Davis P W. Cavity growth mechanism during creep. Act Melt, 1966, 14(9): 1138-1140.

[11] Lemaitre J.&Chaboehe. J.L. Aspect phenomenologique de la Rupture Par Endommagement. J Mec，Appl, 1978, 2(3): 317-365.

[12] Belloni, G., Bernasconi, G., Piatti, G., eds. Creep damage models. Creep Eng Materials and Struct. Proc., Semin. Ispra(Verese)., London, 1979, 195-227.